Evaluation of the Influence of Local Fuel Homogeneity on Fire Hazard through Landsat-5 TM Texture Measures

Article *in* Photogrammetric Engineering and Remote Sensing · July 2010

DOI: 10.14358/PERS.76.7.853

CITATIONS
3

READS
64

4 authors, including:

Cristina Vega-Garcia
Universitat de Lleida
59 PUBLICATIONS **893** CITATIONS
SEE PROFILE

Emilio Chuvieco
University of Alcalá
303 PUBLICATIONS **8,464** CITATIONS
SEE PROFILE

Evaluation of the Influence of Local Fuel Homogeneity on Fire Hazard through Landsat-5 TM Texture Measures

Cristina Vega-García, Jaime Tatay-Nieto, Ricardo Blanco, and Emilio Chuvieco

Abstract

This study analyzed the relationship between landscape homogeneity and fire hazard for a certain area and time period (1984 to 1995), by using logit models. Homogeneity was measured though eight texture measurements computed on visible and NIR bands of Landstat-5 TM data with varying kernel sizes. Several significant models could be developed to predict future burning at the pixel level for the study period. The best spectral band for detecting proneness to burn was TM1, the blue band, and best results were achieved with large window sizes and the Homogeneity texture measure.

Introduction

The spatial and temporal occurrence of wildfire in any area is determined by the geographical arrangement of fuel types and their moisture condition, ignition sources, weather, and topography (Kulakowski and Veblen, 2006). Hazard reduction, or the "treatment of living or dead forest fuels to diminish the likelihood of a fire starting, and to lessen the potential rate of spread and resistance to control" (Merrill and Alexander, 1987), is the preferred, sometimes the only, line of action available to fire managers. Fuel attributes such as dead/alive matter ratios, flammability, canopy bulk density, canopy base height, stand height, and many other physical, chemical and structural variables (arrangement) must be considered in studying fire hazard. Given the difficulty and expense of measuring all required parameters in the field, fire managers usually classify vegetation in a few fuel models for management purposes (Arroyo *et al.*, 2008). Each fuel model is characterized by specific values of fuel depth, heat content of fuel, or moisture of extinction values, for instance, which in turn allow to model fire behavior (Rothermel, 1983).

The managerial application of fuel type classification systems (Anderson, 1982) usually fails to recognize the influence of fuel spatial patterns on fire ignition and propagation. A study by Jia *et al.* (2006) recently pointed at the strong dependency of burned area and fire intensity upon the spatial variability and type of fuels as they are arrayed across the landscape. In Mediterranean countries, past fire history and human activities have greatly modified both fuel type's distribution and condition (Farina, 1998). Pervasive land abandonment processes in Southern Europe Mediterranean countries have generally led to increased fuel loads and greater landscape homogeneity, which has been put forward as a relevant factor in the increment of fire incidence in these countries (Moreira *et al.*, 2001; Romero-Calcerrada and Perry, 2002; Vega-García and Chuvieco, 2006).

In the evaluation of fire hazard through fuel type classification in the Mediterranean, large tracks of land may be classified as just one fuel type, posing a very serious problem when management must efficiently place costly prevention actions. Management must be spatially efficient because fuel treatments for hazard reduction are very expensive, a common problem to all Mediterranean mountainous areas. Additional spatial information is needed, with a good coverage at the landscape level, beyond the fuel type.

Remote sensing techniques have proven to be very useful for fuel type classification and mapping (i.e., Riaño, 2002; Burgan *et al.*, 1998), as well as to monitor fuel status such as dead or live fuel moisture content (i.e., Chuvieco *et al.*, 2004), but they have rarely been used for measuring specific geographical patterns of fuel arrangements, which are potentially relevant in the wildfire process, such as horizontal continuity (homogeneity). Recent studies (Andersen *et al.*, 2005; Jia *et al.*, 2006; Kayitakire *et al.*, 2006; Mutlu *et al.*, 2007' Riaño *et al.*, 2003b; Saatchi *et al.*, 2007; Skowronski *et al.*, 2007) have focused on airborne scanning laser systems (lidar, SAR) or high-resolution satellite data (QuickBird, Ikonos-2) to estimate the spatial distribution of forest fuel types and parameters (biomass, fuel load, crown bulk density) and local forest structure (fractional cover, tree height, basal area), but these important tools for wildfire management are not yet available for most management agencies (Skowronski *et al.*, 2007) and present coverage problems for large areas. On the other hand, the Landsat program (especially after Thematic Mapper (TM) was launched) has been providing valuable moderate-resolution land-cover data for over 30 years, allowing the historical study of many terrestrial processes (Boucher *et al.*, 2006;

Cristina Vega-García and Ricardo Blanco are with the University of Lleida, Avda Alcalde Rovira Roure 198, E-25198 Lleida, Spain (cvega@eagrof.udl.es).

Jaime Tatay-Nieto is with the Boston College, School of Theology and Ministry, 140 Commonwealth Avenue, Chestnut Hill, MA 02467 and formerly with the University of Lleida, Lleida, Spain.

Emilio Chuvieco is with the Department of Geography, University of Alcalá, C/Colegios 2, 28801 Alcalá de Henares, Spain.

Photogrammetric Engineering & Remote Sensing
Vol. 76, No. 7, July 2010, pp. 853–864.

0099-1112/10/7607–0853/$3.00/0

Helder *et al.*, 2008), and characterization of both forest stand attributes (i.e., Franklin *et al.*, 2003) and fuels (i.e., Riaño *et al.*, 2002). This data source was chosen for our study.

Historical fire occurrence has been modeled before in the Mediterranean and elsewhere, usually from fuels, weather, topographic and geographic or socioeconomic factors input into a dedicated GIS (i.e., Vega-García *et al.*, 2008; Zhai *et al.*, 2003), often using satellite data to map important parameters of wildfire risk (i.e., Chuvieco, 2003; López *et al.*, 2002). Recent studies by Lozano *et al.*, (2007 and 2008) included several spectral indices (Normalized Difference Vegetation Index, Normalized Difference Moisture Index, Normalized Burned Ratio, and Tasseled Cap Transformation features on Landsat data) together with other topographic and geographic data in their yearly models of fire occurrence.

All these valuable approaches to fuel typing and the fire occurrence prediction problem using remote sensing data remain "vertical", in the sense that they lack a specific consideration of the influence of the surrounding fuel landscape pattern on local fire occurrence. Since fuel units in a landscape rarely burn in isolation, the spatial pattern of fuels around a fuel unit (pixel) does matter. In fact, landscape configuration measured through different indices (patch density, mean patch size, and Shannon diversity index) was found to be an important parameter in wildfire occurrence before (Lloret *et al.*, 2002). The studies by Lozano *et al.* (2007 and 2008) found a high explanatory power for a variable measuring heathland frequency in a 7 × 7 Landsat TM pixel kernel, but the authors referred to this variable as "describing vegetation type," and did not comment on the contextual value of the information and the obvious implications for fire proneness in a pixel surrounded by a highly hazardous fuel class.

A previous study in the Alto Mijares area, in Spain, suggested that local homogeneity alone could be used to predict future fire occurrence within a 15-year period with a 65 percent accuracy, in small areas (30 m × 30 m Landsat pixels) (Vega-García and Chuvieco, 2006). Local homogeneity was evaluated through eight texture measurements (Angular Second Moment, Homogeneity, Correlation, Contrast, Dissimilarity, Entropy, Mean, Standard Deviation) (Conners and Harlow, 1980; Haralick *et al.*, 1973; Haralick, 1979) applied to the near infrared (NIR) bands of four Landsat images, with a 25 × 25 kernel size for computation.

The potential influence of a different kernel size or an alternative band selection on further improving the predictions remained unexplored in the Vega-Garcia and Chuvieco (2006) paper, so the goal of the present study was to evaluate the influence of kernel size and Landsat-5 TM band selection on the capability of the same eight texture measures to estimate probability of pixel burning within a 12-year prevention planning period, in the same study area. It must be noted, though, that it was not the goal of this study to develop predictive models of fire occurrence for the area, which would necessarily include other factors besides fuel homogeneity. The goal was to test the relative explanatory value of eight texture measures on fire occurrence prediction, when their computational parameters varied, with a view to a future inclusion of more effective landscape homogeneity variables into broader models.

By doing so, we focused on the spatial arrangement of fuels around a pixel and intended to evaluate the influence of local conditions on its proneness to burn. The relationship between the fuel type and the Landsat spectral and spatial characteristics of the top layer of the vegetation canopy had been explored by other authors (i.e., Burgan *et al.*, 1998; Riaño *et al.*, 2002; Arroyo *et al.*, 2008). Our interest was in the local spatial pattern of the remotely sensed vegetation canopy structure not only because canopy structure contributes to fuel type classification (a relationship used in the past to produce fuel type maps), but because it also determines fire spread. Given similar fuel types and general high hazard conditions in many Mediterranean areas, we hypothesized that horizontal continuity of fuels (fuel homogeneity) aggravate the fire spread probability and the general high hazard. Local spatial pattern influences the probability that a pixel is burned: higher homogeneity implies more similar vegetation structures are repeated locally, producing higher continuity in the already hazardous Mediterranean canopy and favoring the spread of fires.

In the development of an invertible reflectance model for conifers, Li and Strahler (1985) found that interpixel variance was related to canopy structure: size, shape and spacing of trees. Woodcock and Strahler established in 1987 that at the spatial resolution of TM images, local image variance is relatively high for forested environments, suggesting that information-extracting techniques utilizing texture are appropriate for this sensor. Canopy spatial patterns that determine local fuel homogeneity can be measured using texture analysis based in the Grey-Level Co-Occurrence Matrix (Haralick, 1979), and this fact has long been exploited by remote sensing. Other authors have used texture indices to measure the effects of fire on landscape pattern (Chuvieco, 1999). By using texture to measure the spatial pattern of the remotely sensed vegetation canopy around a pixel (fuel homogeneity), we made it a surrogate variable for fire contagion likelihood and proneness to burn.

This study purposely dealt with fuel hazard and not with other variables in the fire environment, because fuels may be modified by management, as stated before. If we can identify higher-hazard-homogeneous areas through a simple method that does not involve extensive field work (i.e., texture in remote sensing), the results would greatly help managers devising landscape-level strategies for hazard reduction.

Materials and Methods

Abundant digital information on topography, vegetation (fuels), and fire history was available for the rural and mountainous Mediterranean area of the Alto Mijares (Castellón, Comunidad Valenciana) from the study by Vega-García and Chuvieco (2006). In this interior area of 672.3 km^2, fire behavior Fuel Model 4 (Anderson, 1982; Rothermel, 1983), covered roughly 70 percent of the coarse-grained landscape created by land abandonment since the 50's. Stands of mature shrubs and closed pine stands with flammable foliage are typical candidates for this model, the most hazardous, in which fast-spreading intense fires "involve the foliage and live and dead fine woody material in the crowns of a nearly continuous secondary overstory"(Anderson, 1982). Mean patch size for dense shrublands and Aleppo pine forest belonging to this model in the Alto Mijares reached 11.5 and 13 ha, respectively, but size variability was very large (Vega-García, 2003).

The field-based fire history database of fires larger than 5 ha in the study by Vega-García and Chuvieco (2006) provided the dependent variable: if the pixel was burned in the 1984 to 1995 period was coded as Y = 1, if not, it was coded as Y = 0. The study period from 1984 to 1995 was selected because by 1984 the human population was at the lowest in the Alto Mijares, and most fuel load accumulation had already taken place. Forest structure changed very little, since no harvesting took place, and there was no reforestation. Landscape dynamics had become fire-driven (Vega-García, 2003), but over this period fire suppression resources remained stable. This period was the worst in the fire history of the Alto Mijares, both in number of fires and in area burned, and preceded in time a Fire Prevention Plan for the region (Tragsatec, 1996) which would later imply the construction of an extensive fuelbreak network. Figure 1

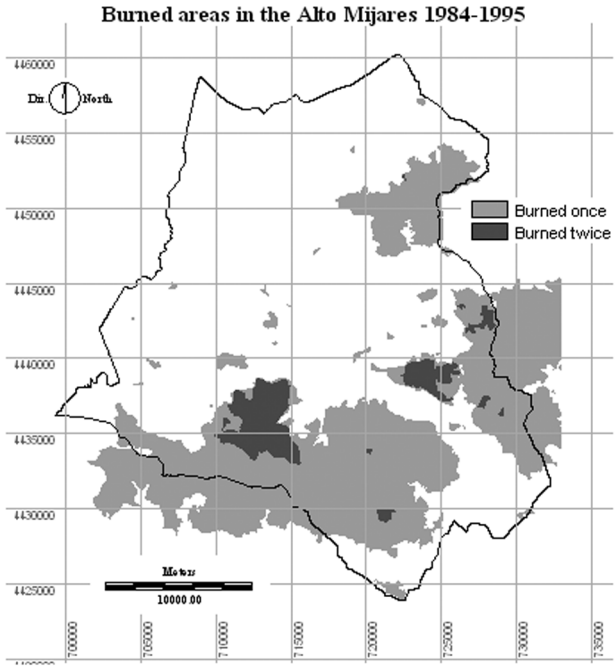

Figure 1. Perimeters of fires over 5 ha in the period 1984 to 1995 in the Alto Mijares study area.

displays the location of the 38 fires larger than 5 ha occurred in the Alto Mijares between 1984 and 1995. Out of the 38 fires in the period only nine were larger than 200 ha. One fire burned more than 19,000 ha in 1994. This size variability, common to any fire regime, suggested that a sufficiently wide range of fire conditions were accounted for. There were some relatively wet years and some relatively dry years in the study period, but none out of the ordinary for this Mediterranean area. After 1995, very few fires have taken place, but it is expected that conditions similar to past will develop in the near future (after 2010), based on observed vegetation recovery patterns and known vegetation dynamics in the region (Roselló-Gimeno, 1994).

A cloud-free Landsat-5 TM image (path/row 199/032) acquired the 19 July 1984, and geometrically corrected (UTM Zone 30T, European Datum 1950) with control points and a nearest-neighbor algorithm, was converted to radiance values using standard calibration values (Price, 1987). The dark-object algorithm by Chavez (1996) was used to remove atmospheric dispersion. The c-correction method (Teillet *et al.*, 1982) modified by Riaño *et al.* (2003a) was applied to the image to remove shadowing effects caused by the abrupt topography (32 percent average slope). Figure 2 displays bands TM3 and TM4 after corrections.

Eight texture measures or indices defined by Haralick *et al.* (1973), Haralick (1979), and Conners and Harlow (1980) (Table 1) were then calculated for each pixel (30 m $\times$ 30 m) in bands TM1, TM2, TM3, and TM4 of the 1984 reflectance image, corresponding to the Blue, Green, Red, and NIR, respectively, regions of the spectrum. Angular Second Moment, Homogeneity, Correlation, Contrast, Dissimilarity, and Entropy are considered the six most relevant texture measurements for remote sensing data analysis out of the fourteen originally defined by Haralick *et al.* (1973) (Kayitakire *et al.*, 2006). Mean and Standard Deviation values have also been used before in texture assessment (Tso and Mather, 2001; Tuominen and Pekkarinen, 2005; St-Louis *et al.*, 2006). We used the TEX command in the PCI software (PCI, Inc., 1997) for computing these texture indices. For any local window of a certain size (centered at a reference pixel), the

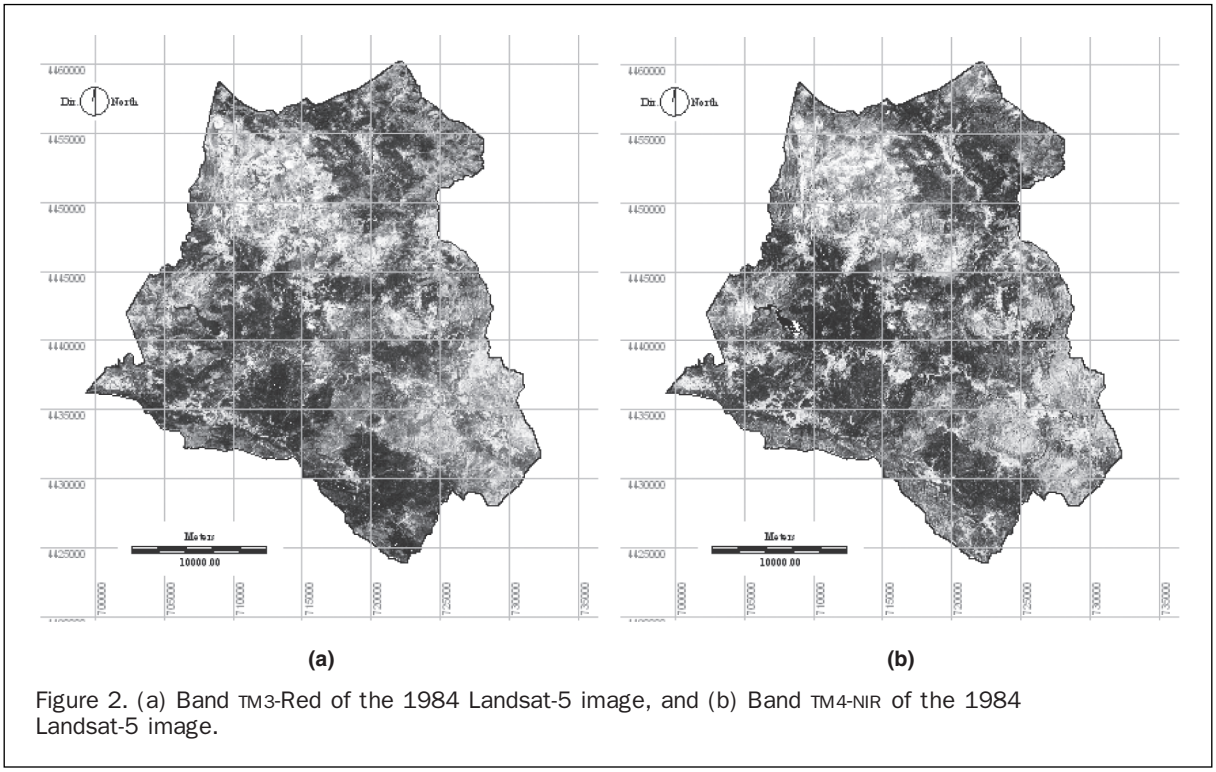

Figure 2. (a) Band TM3-Red of the 1984 Landsat-5 image, and (b) Band TM4-NIR of the 1984 Landsat-5 image.

TABLE 1. DEFINITION OF TEXTURE INDICES

Variable	Description
Homogeneity*	SUM (i,j=0,N−1)(P(i,j)/(1+(i−j)**2))
Contrast	SUM (i,j=0,N−1)(P(i,j)*(i−j)**2)
Dissimilarity	SUM (i,j=0,N−1)(P(i,j)*|i−j|)
Mean	SUM (i,j=0,N−1)(i*P(i,j))
Standard Deviation	SQRT (Var_i), where Var_i = SUM(i,j=0,N−1)(P(i,j)*(i − Mean_i)**2)
Entropy	SUM (i,j=0,N−1)(−P(i,j)*LOGe(P(i,j))), assuming that 0*LOGe(0) = 0
Angular Second Moment*	SUM (i,j=0,N−1)(P(i,j)**2)
Correlation*	SUM (i,j=0,N−1)(P(i,j)*(i−Mean_i)*(j−Mean_j))/SQRT(Var_i*Var_j)

*The values of these variables increase with homogeneity in the local window

command computes texture measurements derived from the co-occurrence matrix of reflectance values (the Grey Level Co-occurrence Matrix (GLCM) or grey-tone spatial-dependence matrix after Haralick *et al.*, 1973), a two-dimensional histogram of digital (reflectance) counts for a pair of adjacent pixels which are separated by a fixed spatial relationship (the displacement value, δ) and an angular spatial relationship (the direction parameter, θ = 0, 45, 90, and 135 degrees). The GLCM matrix of relative frequencies approximates the joint probability distribution of any such pair of pixels in the window. Haralick *et al.* (1973) stated that the GLCM "describes how often one gray tone will appear in a specified spatial relationship to another grey tone on the image." In our case "grey tones" were reflectances and "images" were windows of variable size placed in order over all pixels in each band of the 1984 image. For a good approximation, the number of different digital values must be relatively few, and window size must be relatively large (PCI, Inc., 1997). A study by Tuominen and Pekkarinen (2005) experimented with different digital ranges for Angular Second Moment, Contrast, Correlation, Entropy and Homogeneity to relate texture measurements and forest stand volume, finding that best correlations were achieved with 14 to 16 different digital classes in ten out of fifteen models. Marceau *et al.* (1990) found that this quantization level had very little impact in texture measurements performance for improving land cover classification. For this reason, we reduced the original range of reflectance values to 16 classes, using an adaptive nonlinear scaling method (PCI, Inc., 1997) which preserved the shape of the original histogram and was robust against a few extreme outliers in the input reflectance image of 1984.

A key parameter in the texture measurements is the size of the window (kernel) from which the texture indices are computed. Marceau *et al.* (1990) tested the influence of seven window sizes on land-cover classification accuracy and found that for each land-cover a window size existed that maximized classification accuracy. There are not objective methods to compute the ideal size of this kernel. Many authors do not justify the choice of a window size, i.e., 3 × 3 on Landsat and SPOT data for estimating forest stand attributes in Cohen and Spies (1992). Frequently, trial and error methods are used and several kernel sizes are computed and compared (Kayitakire *et al.*, 2006). In this study four kernel sizes were used for computation of the texture indices: 5 × 5, 15 × 15, 25 × 25, and 35 × 35 pixels. These kernel sizes allowed the evaluation of fuel conditions in squared areas around each pixel ranging from its near-neighborhood to relatively wide regions, measuring respectively 2.25, 20.25, 56.25, and 110.25 ha. Since mean patch size for dense shrublands and Aleppo pine forest (Fuel Model 4 in the Alto Mijares) reached on the average 11.5 and 13 ha, respectively (Vega-García, 2003), kernel size was also considered to be theoretically related to intra-patch conditions for the smaller kernel and to inter-patch condition for the larger ones.

A decision to use the three visible and the near-infrared band from the Thematic Mapper sensor was based in the statement by Haralick *et al.* (1973) and Haralick (1979) about the inextricable relationship between tone and texture in any image. Tonal properties influence texture measurements results. Since different bands in a Landsat image exhibit varying reflectance (tonal) values, texture indices would vary accordingly with band selection. Given the current state of most space-based Earth observation programs and the increasing availability of multi-spectral and hyper-spectral images from different sensors, we considered that a discrimination of at least the spectral regions of interest among the blue, green, red, and infrared dominions would facilitate future studies of fire proneness based on local homogeneity measures. Bands TM5 and TM7 (shortwave infrared and mid-infrared) were not used because water contents were relatively variable from year to year and seasonally in the area (for instance, 1991 was a wet year with precipitation a bit over 600 mm, 1995 was a dry year with a bit less than 400 mm). Because the Mediterranean vegetation in the area is well adapted to normal weather conditions, spectral signatures did vary very little between years, especially in bands TM1 (blue), TM2 (green), and TM3 (red). An analysis using four dates (1984, 1991, 1995, and 1998) in Vega-García (2003) exhibited slight changes with yearly conditions by bands TM4 (near-infrared), TM5 (shortwave infrared), and TM7 (mid-infrared), making them less desirable for our study, since we were looking for stability in the data, reflecting structural characteristics, not inter-annual variation in vigor or water content. We considered band TM4 should not be excluded because of its general importance in vegetation studies.

Therefore, local homogeneity was calculated for four kernel sizes, for each of the four TM bands, and for each of the eight texture measures, rendering 128 texture images of the Alto Mijares area for analysis (4 kernels × 4 bands × 8 texture indices). Figure 3 illustrates two examples of these spatial operations.

The displacement parameter was set to one (δ = 1), in order to test for homogeneous contiguity conditions in fuels. Also, studies by Tuominen and Pekkarinen (2005) and Kayitakire *et al.* (2006) suggested that short lags (a few meters) performed better in forest stand features extraction. The direction parameter (θ) was held invariant, since our previous knowledge of the area did not indicate the existence of preferential fire spread patterns. Kayitakire *et al.* (2006) found the direction parameter had minimal effects in modeling forest structure parameters, though they used high resolution Ikonos-2 data. Directional invariance

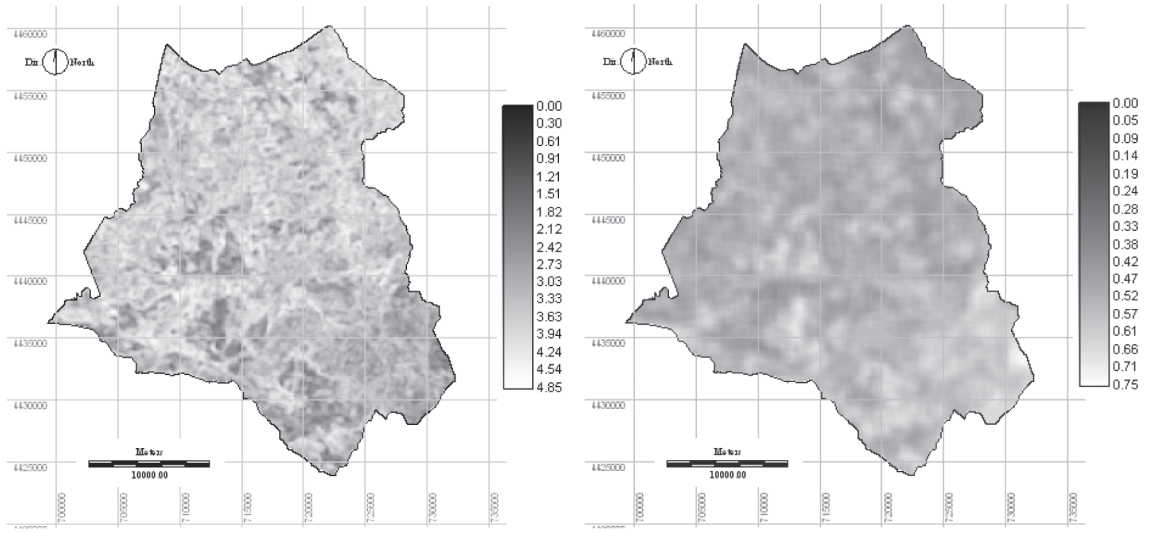

Figure 3. (a) Entropy texture measure computed on TM1-Blue band with a kernel size of 15 pixels × 15 pixels, and (b) Homogeneity texture measure computed on TM1-Blue band with a kernel size of 35 pixels × 35 pixels.

was achieved by computing the GLCM at four directions, horizontal, vertical, and diagonal (0, 45, 90, and 135°), and summing them before texture calculation. A detailed definition of each texture measure based on GLCM computation may be found in the paper by Haralick *et al.* (1973) where the textural features were originally defined.

One percent (10,856 observations) of all pixels in each image was randomly sampled for statistical analysis. Pixels were sparsely distributed over the study area (672.3 km^2), apart from each other, so that the kernels applied for texture computation would not overlap, and spatial correlation problems would be basically avoided. Data was randomly split in two datasets, 80 percent of the data (8,685 pixels, including 3,331 fire observations and 5,354 no-fire observations) were used for model building and 20 percent (2,171 pixels, including 864 fire observations and 1,307 no-fire observations) were separated for validation purposes. Sampling was avoided in all non-combustible areas (urban areas, water, roads, irrigated and fallow land) which had been previously identified by Vega-García (2003).

Local homogeneity (texture) variables were investigated through descriptive statistics, and a general correlation analysis was performed among all variables. Very high correlation values were to be generally expected among all variables, due to their mode of generation from same or similar co-occurrence matrices and bands close by in the visible and near-infrared regions of the spectrum, belonging to a same image. Due to this fact, the statistical modeling of the expected relationships between future fire occurrence and local homogeneity would admittedly suffer from multicollinearity problems, if all independent variables were input into the models. But this was not intended, since the purpose of the study was specifically the evaluation of kernel size and band selection factors in the explanatory capability of the different texture measures. The stated objective required to build univariate models anyways, to compare the performance of the different texture measures as a function of band selection or window size.

The dichotomous nature of the dependent variable (burned/unburned in the next 12 years) led us to select the logit model (Cox and Snell, 1989; Ben-Akiva and Lerman, 1985) as best fitted for our analysis. The logit model has been frequently used for fire occurrence prediction (Loftsgaarden and Andrews, 1992; Vega-García *et al.*, 1995; Cardille *et al.*, 2001; Preisler *et al.*, 2004). Its advantages have been reviewed elsewhere (Vega-García *et al.*, 1995). According to this model, the probability P_i that a given pixel i will burn is given by:

$$P_i = P(Y = 1) = \exp(Z_i)/(1 + \exp(Z_i)) \quad (1)$$

where Z_i is a function of an independent texture variable X_i, and b_0 and b_1 are the parameters to estimate, usually through maximum likelihood methods (Maddala, 1988):

$$Z_i = b_0 + b_1 X_i. \quad (2)$$

The probability that a pixel will not burn may be computed subtracting Equation 1 from 1 and simplifying:

$$1 - P_i = P(Y = 0) = 1/(1 + \exp(Z_i)). \quad (3)$$

By dividing Equations 1 and 3 and applying natural logarithms to both sides of the equation it is possible to obtain the log-odds ratio of the two possible outcomes as a linear function of any independent texture variable X:

$$\ln(P_i/(1 - P_i)) = Z_i = b_0 + b_1 X_i. \quad (4)$$

For this study, 128 logit univariate models were developed and tested, one for each of the texture measure-band-kernel combination (X_i). Modeling was carried out with the LOGISTIC procedure of the SAS v. 8.2 software (SAS Institute, Inc., 1999).

Best models were evaluated and selected by means of both their predictive capability and goodness of fit to the data. For the latter, the Hosmer-Lemeshow goodness of fit test (Hosmer and Lemeshow, 1989) was used. Predictive

capabilities were tested using a 2 × 2 classification table of observed and predicted responses (SAS Institute, Inc., 1999). For the best models, the ROC (Receiver-Operating Characteristic) plot (Stephens and Finney, 2002) was generated and analyzed to determine the best probability level or cut-off point to segregate observations into likely or unlikely events (future pixel burn yes/no). The c-value (area under the ROC curve) was also consulted as a measure of predictive effectiveness and model fit (Lozano *et al.*, 2007). Estimated parameter significance was evaluated with the Chi square test and Wald statistic (the squared ratio of the B_i coefficient by its standard error) (Ben-Akiva and Lerman, 1985), which is a test of the null hypothesis that a particular coefficient is zero (Wald Chi-square).

Results

The correlation analysis confirmed the need to build univariate models in this case. All texture variables (128) were very highly correlated. In all cases texture variable correlations were higher than 0.4, and in the majority of cases were higher than 0.7 in absolute value.

Several significant models could be developed to predict future burning at the pixel level for the study period (1984 to 1995), based in local homogeneity values measured on 1984 data (the Landsat TM image) through the texture measures of this study. However, conditions of estimated parameters significance ($p < 0.05$) with significant goodness of fit (Hosmer-Lemeshow, 1989) and c-value >0.6 were achieved only by five models out of 128 (Table 2).

Band TM1 (Blue) was predominant in this group with four models, the fifth being based on band TM3 (Red). Homogeneity (four models) was the leading texture index, followed by Entropy (1 model). Angular Second Moment, Contrast, Correlation, Dissimilarity, Standard Deviation, and Mean were absent from this group of selected models. Signs of the significant estimated parameters were as expected according to the theoretical definition of the texture measurements; Homogeneity showed a positive relationship with proneness to burn, and this relationship was negative for Entropy. All window sizes were present, but the larger seemed to be associated to better performances in the best models.

Only three models obtained a c-value (area under the ROC curve) over 0.65. The best three logit models corresponded to the Homogeneity index computed on band TM1-blue with the larger window sizes, 35 × 35, 25 × 25 and 15 × 15 pixels, and by that order. The significance tests for the estimated parameters in the best logit model (c-value 0.71, Chi-square 11.95, $p = 0.1531$) are presented in Table 3.

The predictive capability of this model reached a 67.9 percent total percentage correctly predicted at the midpoint (0.5) value of the logistic function, which is customarily applied in most analysis (Table 4). The model predicted better the pixels that would not burn (85 percent correct), than those which would be burned (41 percent). However, a different probability level could be used (Jamnick and Beckett, 1987) depending on management objectives, e.g., to reduce false alarms, or improve detection of fire-prone areas. By selecting a probability level of 0.4, for instance, the total percentage correctly predicted decreased just slightly, to 66.3 percent, but correct predictions in fire-prone/no-fire-prone areas were more balanced, 58.9 percent and 70.8 percent, respectively.

Discussion and Management Implications

Several significant univariate logit models were built to explain future fire occurrence in the Alto Mijares based on several texture measures of landscape homogeneity. Overall accuracy of the best model (66 to 68 percent) was similar to those found by other authors (e.g., 68 to 72 percent: Lozano *et al.*, 2007; 65 percent: Vega-García and Chuvieco, 2006), but this model contained just one variable, Homogeneity, with a positive sign in the significant estimated coefficient. This model supported the relationship between homogeneity conditions of fuels in a wide local window (35 pixels × 35 pixels; 110.25 ha) and wildfire occurrence. The relationship found suggests that important canopy structural characteristics can be discriminated from surrogate measures such as texture (St-Louis *et al.*, 2006), in this case, fuel continuity.

TABLE 2. VALUES OF **c** AND **p** PARAMETERS FOR THE BEST MODELS

Band	Texture M.	kernel size	c (ROC curve)	p (H-L)
band TM1	HOMOG	35×35	0.71	0.1521
band TM1	HOMOG	25×25	0.698	0.4452
band TM1	HOMOG	15×15	0.679	0.2336
band TM3	HOMOG	5×5	0.642	0.1322
band TM1	ENTROPY	15×15	0.606	0.4474
band TM3	DISIM	5×5	0.569	0.3364
band TM1	DISIM	5×5	0.564	0.4240
band TM3	ENTROPY	5×5	0.563	0.2299
band TM1	ENTROPY	5×5	0.556	0.0797
band TM2	ENTROPY	5×5	0.556	0.6692
band TM4	ENTROPY	35×35	0.552	0.2138
band TM4	ENTROPY	25×25	0.544	0.1389
band TM4	CORREL	5×5	0.523	0.3017

TABLE 3. ESTIMATED PARAMETERS: VALUES AND WALD CHI-SQUARE SIGNIFICANCE TESTS

Parameter	DF	Coefficient	Standard Error	Wald Chi-square	Pr > ChiSq
Intercept	1	−9.7079	0.2972	1067.255	<.0001
Homog35TM1	1	16.7408	0.5349	979.4992	<.0001

TABLE 4. CLASSIFICATION TABLE FOR THE BEST LOGIT MODEL, AT DIFFERENT PROBABILITY LEVELS

Probability Level	Correct		Incorrect		Percentages				
	Event	Non-Event	Event	Non-Event	Correct	Sensitivity	Especificity	False Posit.	False Negat.
0.400	1961	3793	1561	1370	66.3	58.9	70.8	44.3	26.5
0.500	1356	4541	813	1975	**67.9**	40.7	84.8	37.5	30.3
0.600	847	4960	394	2484	66.9	25.4	92.6	31.7	33.4

Band Selection

Model results indicated that the best spectral band for detecting proneness to burn was TM1, the blue band; although the TM3 (Red) band may also be an important spectral region for estimation of fire proneness. These results seemed to be at variance with other studies, which have generally favored *a priori* spectral indices computed from the NIR and red bands (e.g., Lozano *et al.*, 2007), but they did agree with the design characteristics of the Landsat TM bands. TM2 was designed to detect green reflectance from healthy vegetation, TM3 for chlorophyll absorption in vegetation, and TM4 for detecting near-IR reflectance peaks in healthy green vegetation; but the fact is that TM1 was designed for distinguishing forest types and for soil-vegetation differentiation (Earth Observation Satellite Company, 1994). The lowest reflectance values for vegetation occur in the blue waveband (Tso and Mather, 2001) and bare soil reflectance is greater than that of the vegetation in the visible bands. Both forest types and soil-vegetation patterns examined in the blue spectral region should be expected to be directly related to fuel type and distribution, and consequently, to fire hazard. Also, the blue band is the most influenced by dispersion, which could produce higher shadow variability than in other bands.

The study by Lozano *et al.* (2007) found good results for spectral indices based on SWIR (shortwave-infrared, TM7) and MIR (mid-infrared, TM5) wavelengths, which they attributed to their relationships with moisture content in vegetation and soil and a better capability than visible bands to penetrate thin clouds and smoke. Tasseled Cap Wetness-based models, which included the visible bands, had the best goodness-of-fit, while the Greenness factor showed little explanatory value.

These results suggest a need to critically examine the best spectral domain for fire occurrence prediction in future studies. Spectral regions related to forest type discrimination could be more useful for hazard evaluation and wildfire occurrence prediction in fire-prevention time frames (several years) than bands in the domain designed for vegetation activity monitoring and biomass estimation, which are probably more useful in fire-suppression time frames (several days); but this aspect was not covered in this paper.

Window Size

All window sizes were present in the prediction models, but only one model had the 5×5 kernel, in the same order of magnitude than the results by Lozano *et al.* (2007) regarding the good predictive power of a percentage-of-heath contextual variable computed with a 7×7 kernel. Best models, though, exhibited large window sizes, an in descending order within the same spectral domain and texture measure, which suggested a clear pattern in the Alto Mijares where local fire proneness increases with areas of surrounding homogeneous fuel of at least 100 ha.

Most texture measures exhibited somewhat different values for the small kernel size (5 pixels $\times$ 5 pixels; 2.25 ha) than for the rest. Since fuel mean patch size was 11 to 13 ha in this landscape, the difference in values may be explained by the fact that the 5×5 kernel was mainly linked to intra-patch texture, while the other kernels (>20.25 ha) were connected to inter-patch texture. The small window size would capture the influence of the internal structural variation of each fuel type patch on the wildfire process, while the larger windows would be associated to fuel type pattern in the landscape.

Texture Index

The predominant texture index in the significant models was Homogeneity, but Entropy was selected in one model. Correlation and Entropy were found the most relevant for land-cover classification by Rao *et al.* (2002). Homogeneity was selected in the best model, however. Homogeneity was found to perform well in forest age discrimination on Ikonos data by Franklin *et al.* (2001), but no other texture measurements were evaluated by these authors.

It is remarkable that Angular Second Moment, Contrast, Mean, and Standard Deviation were absent from the group of selected models. These results apparently differed from findings in Vega-García and Chuvieco (2006), where Angular Second Moment and Standard Deviation were found to be very important variables for fire prediction. However, the models in that study were artificial neural networks and they were not univariate, a pool of texture measures would always be input into the networks. When input to the nets, Angular Second Moment would undergo a linear transform in most cases, and Standard Deviation would be transformed by a hyperbolic transfer function. Therefore, it is important to indicate that the explanatory value of independent variables is determined by the modeling technique, in our case, the logistic regression analysis. Other techniques may be able to detect non-sigmoid patterns in the data and select other texture measurements. In any case, Angular Second Moment and Homogeneity were variables very highly correlated and both increased with grey-level homogeneity in the local window. Both Homogeneity and Angular Second Moment were recommended by Solberg (1999) as best for forest map revision.

Why would the Homogeneity index be the most informative in this particular case? The information content of each measure depends "on the type of image analyzed with regards to the spectral domain, spatial resolution and characteristics of the sensed objects (dimension, shape and spatial distribution)" (Kayitakire *et al.*, 2006). Here, all measurements pertained to the same image and, therefore, characteristics of sensed objects, the fuel patches, were the same. Though absolute values of the texture measures do not have a physical meaning by themselves, it was our stated goal to particularly evaluate the relative influence of kernel size and Landsat-5 TM band selection on the values and the capability of the texture measures to estimate probability of pixel burning. By keeping spectral domain invariant and varying the kernel size, local influence on information content could be inferred, and alternatively, by keeping kernel size fixed spectral domain effects could be assessed.

The plots of mean values for each measure-band-kernel size combination contributed to clarify the favorable results for Homogeneity, and also for Entropy, second to it. Figure 4 shows the variation of mean values of Homogeneity and Entropy, with spectral band and window size.

The analysis of these plots provided evidence that both Homogeneity and Entropy behaved as could be theoretically expected according to their definitions. Most of the Alto Mijares area is covered by Fuel Model 4, but this type may include in fact several vegetation classes (Vega-García, 2003), and the topography is highly fractured, causing complex local patterns. Even though spectral vegetation characteristics in relation to topographic attributes vary across geographic space and spatial scales (Deng *et al.*, 2007), increased window size should reveal more heterogeneity for all texture measures in the Alto Mijares. The texture measures were defined as functions of the statistical distribution of the spatial relationships of grey-level (reflectance) properties. Should the textures be coarse, the statistical distribution would change little with distance; should they be fine (heterogeneous), the distribution would change rapidly with distance (Aksoy and Haralick, 1998). The fuel patterns in the Mijares area could be defined as relatively coarse at the Landsat image resolution, so they should be expected to become more heterogeneous with window size but with changes of small magnitude in texture values.

Homogeneity and Entropy values did agree with theoretical trends. The fact that their plots exhibited an asymptotic trend with larger window sizes also agreed with findings by Kayitakire *et al.* (2006), denoting that the texturing objects sizes of interest with regard to fuel hazard (patches) were reached at these window sizes. Information content would be similar at the three larger window sizes, explaining the comparable results in their models, for the blue band. The blue band in the Homogeneity plot clearly separated from the rest, indicating a different behavior of this measure in this spectral region.

We concluded that for this Landsat-TM image acquisition conditions and configuration of spatial objects (vegetation canopy/fuel patches), texture explanatory value varied with computational parameters; both band (blue) and kernel size (35 pixels × 35 pixels) played a significant role in determining Homogeneity fitness to describe fuel hazard in this landscape.

Applicability of the Results

Application of the Homogeneity model (blue band, 35 × 35 kernel size) to the validation dataset produced a 67.3 percent total correctly predicted at the midpoint (probability level = 0.5) of the logistic function (Table 5). By selecting a probability level of 0.4, the total percentage correctly predicted slightly decreased to 66.8 percent, but correct predictions in fire-prone/no-fire-prone areas were more balanced, 57.5 percent and 73 percent, respectively. These values were almost identical with those of the model building data (Table 4), indicating a good generalization capability of the model.

Even though this logit model could only be applicable in this study site, for this image and correction techniques, the procedures are simple enough to be applied in other areas where a rapid assessment of fuel hazard allied to homogeneous fuel-model conditions is required. However, since texture is the structural arrangement of surfaces (tonal primitives; Haralick, 1979), it depends on the spatial resolution of the sensor and the size of the homogeneous area being characterized.

Vegetation spectral response is linked to multiple environmental factors (Deng *et al.*, 2007), so if the area over which texture is measured includes several fuel classes, the measures may not be useful (Tso and Mather, 2001).

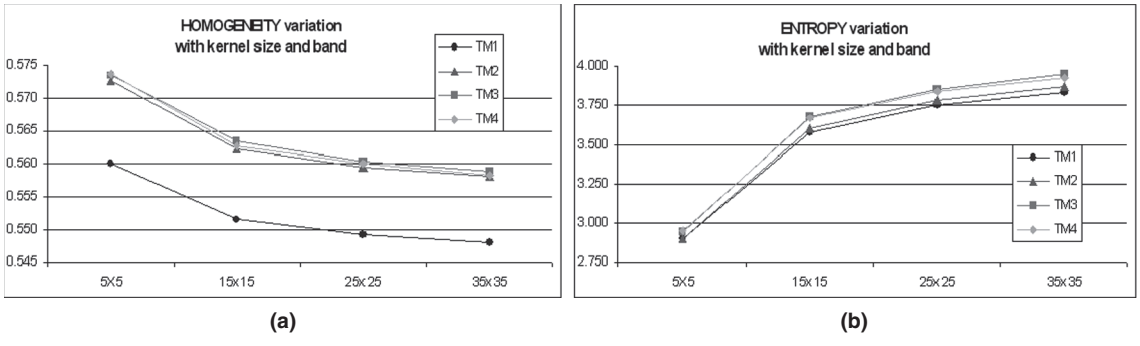

Figure 4. Variation with band and kernel size for texture measurements: (a) Homogeneity, and (b) Entropy.

TABLE 5. CLASSIFICATION TABLE FOR THE BEST LOGIT MODEL, AT DIFFERENT PROBABILITY LEVELS, FOR THE VALIDATION DATA

Probability Level	Correct		Incorrect		Percentages				
	Event	Non-Event	Event	Non-Event	Correct	Sensitivity	Especificity	False Posit.	False Negat.
0.400	497	954	353	367	66.8	57.5	73.0	41.5	27.8
0.500	348	1113	194	516	**67.3**	40.3	85.2	35.8	31.7
0.600	227	1229	78	637	67.1	26.3	94.0	25.6	34.1

The use of this approach would avoid some drawbacks in the use of classified images for fuel hazard evaluation in coarse-grained homogeneous fuel-type landscapes, which may mask local pixel heterogeneity and increase processing time (St-Louis *et al.*, 2006), providing scarce spatial information for fire prevention management.

In order to illustrate the outcome of this process, we produced a map of probability of future wildfire occurrence or proneness to burn for the Alto Mijares study area, by applying the logit model to the Homogeneity image computed on the blue band with a 35 × 35 kernel. Figure 5 displays two maps: the resulting probability map and a fuel model map of the area, originated by a maximum likelihood digital classification based on the six 30 m resolution bands of the TM84 image plus the topographic variables, aspect, slope, and elevation (Vega-García, 2003).

The availability of a fire hazard map derived from a surrogate texture variable as Homogeneity (Figure 5b) can be of help to fire managers facing extensive and expensive silvicultural interventions, helping to more efficiently locate fuel treatments than when they are based on fuel maps such as the one in Figure 5a. Figure 6 shows the 78,760.44 hectares of Fuel Model 4 in the study area, sliced in probability of burn levels (deciles in this case) or categories of fuel hazard, accordingly to the Homogeneity logit model of this study. Examination of this map suggests that a unique opportunity to anticipate and aid fuel treatments within the most hazardous fuel in the Alto Mijares existed in 1984.

In 1996, after the great fires of 1993 and 1994 (32,334 ha in those two years) burned most of the southeast (and a great part of the homogeneous areas), a fire prevention plan was approved for the region based on a fuel type map of 1996 (Tragsatec, 1996). Isolated treatments were performed along roads in the following years, but execution of the main fuelbreak network did not start until recently, i.e., in 2004. Again, application of the best logit model to a Landsat TM image acquired in 1995 and processed identically as the 1984 image (Vega-García and Chuvieco, 2006) could have provided improved information on the homogeneity characteristics of the most dangerous fuels, and aid this planning (Figure 7).

The almost complete absence of large fires in the Alto Mijares in the last years (only a 18 ha fire in 1997 and a 8 ha fire in 2001) may contribute to a perception that not immediate action needs to be taken, but the expectation that a few more years of vegetal succession will drive the landscape to similar hazard conditions to those existing in 1984 still hold, advising that a higher resolution spatial diagnosis tool is needed.

The inclusion of landscape homogeneity variables into models of fire occurrence and in fire prevention planning would allow considering specifically the influence of the surrounding fuel landscape pattern on local fire occurrence, adding more detailed spatial information to the fuel model classification usually employed by managers. These variables may be critical in Southern Europe Mediterranean countries under pervasive land abandonment processes were landscape homogeneity has been put forward as a relevant factor of higher fire incidence.

Conclusions

Homogeneity conditions in forest fuels do have an impact on wildfire occurrence, according to this study. Fuel homogeneity in a wide local window of 110.25 ha around a Landsat-5 30 m pixel was found to increase its probability of burning in a subsequent period of 12 years in the Alto Mijares, in Mediterranean Spain. A significant logit model allowed computing this probability with a 68 percent total percentage correctly predicted based on the Homogeneity texture measure. We concluded that for this Landsat image acquisition, conditions and configuration of spatial objects (fuels) texture explanatory value varied with computational parameters; both band (blue) and kernel size (35 × 35 pixels) determined Homogeneity fitness to describe fuel hazard in this landscape created by land abandonment. The availability of a fire hazard map derived from a surrogate texture variable as Homogeneity can be of help to fire managers facing extensive

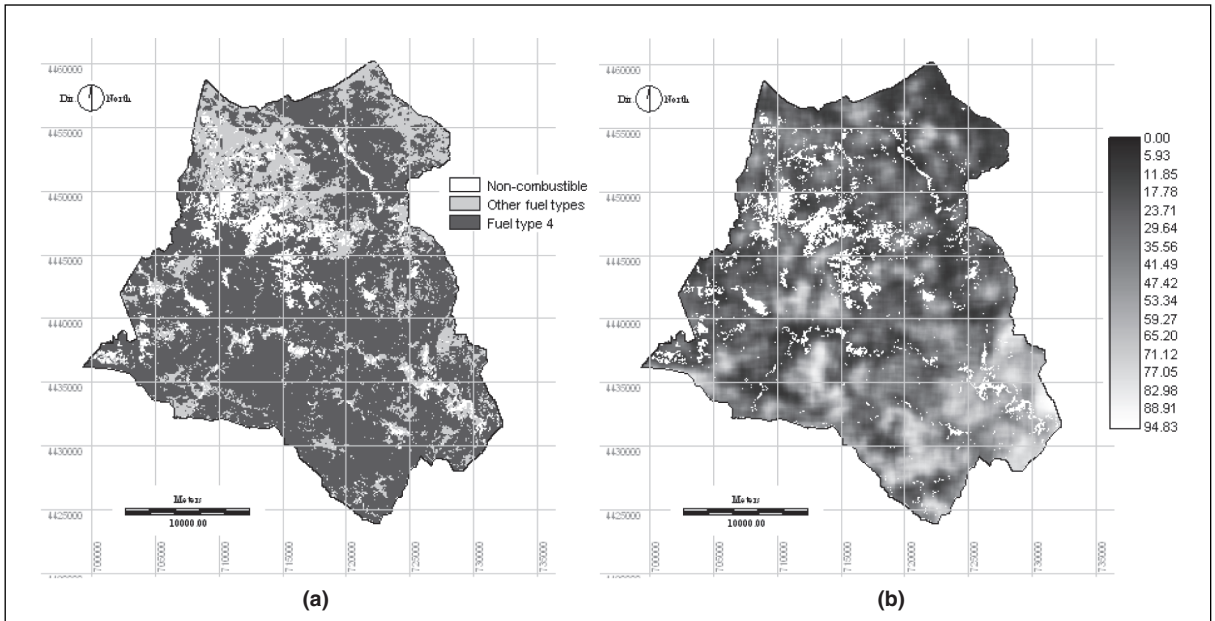

Figure 5. (a) Fuel type map of the Alto Mijares, and (b) Proneness to burn in the same area for the study period 1984 to 1995 (in percentage).

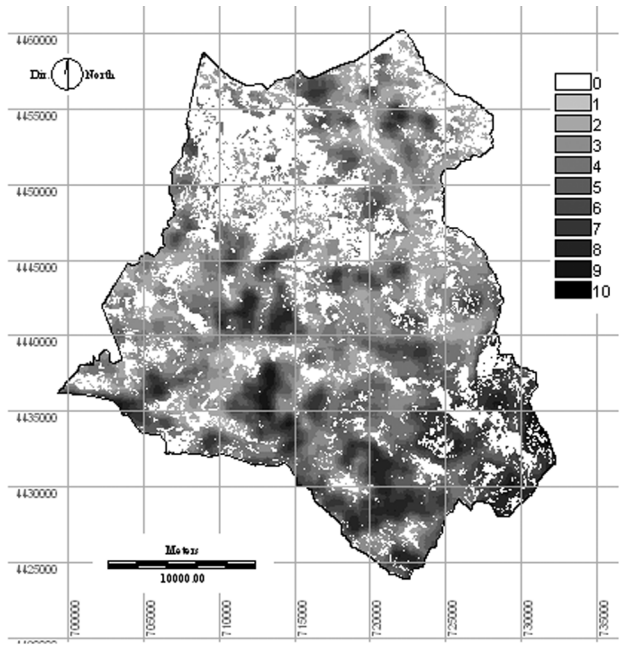

Figure 6. Fuel Model 4 areas within the Alto Mijares reclassified (deciles) accordingly to their proneness to burn in 1984, based on their homogeneity characteristics. Darker areas represent higher fuel hazard.

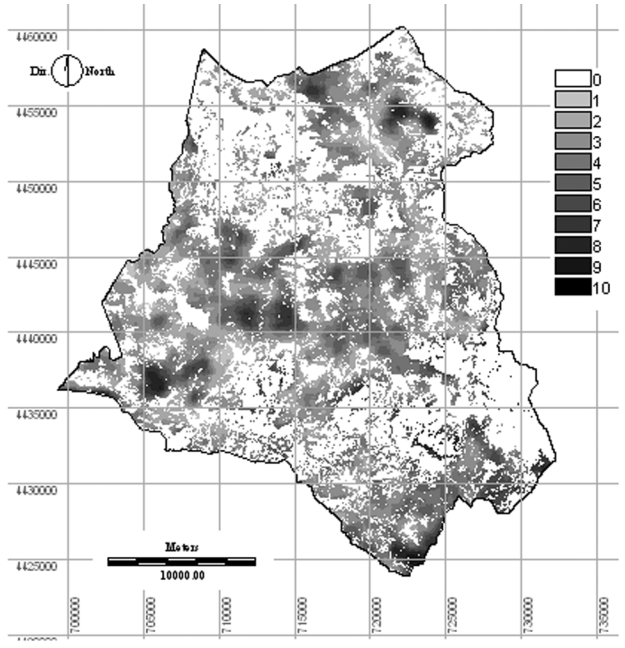

Figure 7. Fuel Model 4 areas within the Alto Mijares reclassified (deciles) accordingly to their proneness to burn in 1995, based on their homogeneity characteristics. Darker areas represent higher fuel hazard.

and expensive silvicultural interventions, helping to more efficiently locate fuel treatments in areas where the usual fuel type mapping does not provide sufficient spatial information to optimize fire management action.

Acknowledgments

We thank the Conselleria de Medio Ambiente, Generalitat de Valencia in Castellón, for supplying historical fire records. Special gratitude is due to the local forest technicians, who helped in the fieldwork and the identification of past fires. We gratefully acknowledge insightful comments from three anonymous reviewers of the PE&RS Journal.

References

Aksoy, S., and R.M. Haralick, 1998. Textural features for image database retrieval, *Proceedings of the IEEE Workshop on Content-Based Access of Image and Video Libraries*, in conjunction with CVPR'98, June, Santa Barbara, California, pp. 45–49.

Andersen, E.H., J.R. McGaughey, and E.S. Reutebuch, 2005. Estimating forest canopy fuel parameters using lidar data, *Remote Sensing of Environment*, 94:441–449.

Anderson, H.E., 1982. Aids to determining fuel models for estimating fire behaviour, USDA Forest Service, Intermountain Forest and Range Experiment Station, *General Technical Report INT-122*, Odgen, Utah, 16 p.

Arroyo, L.A., C. Pascual, and J.A. Manzanera, 2008. Fire models and methods to map fuel types: The role of remote sensing, *Forest Ecology and Management*, 256:1239–1252.

Ben-Akiva, M., and S.R. Lerman, 1985. *Discrete Choice Analysis: Theory and Application to Travel Demand*, The MIT Press, Cambridge, Massachusetts, 390 p.

Boucher, A., K.C. Seto, and A.G. Journel, 2006. A novel method for mapping land cover changes: Incorporating time and space with geostatistics, *IEEE Transactions on Geoscience and Remote Sensing*, 44:3427–3435.

Burgan, R.E., R.W. Klaver, and J.M. Klaver, 1998. Fuel models and fire potential from satellite and surface observations, *International Journal of Wildland Fire*, 8:159–170.

Cardille, J.A., S.J. Ventura, and M.G. Turner, 2001. Environmental and social factors influencing wildfires in the Upper Midwest, *United States, Ecological Applications*, 11:111–127.

Chavez, P.S., 1996. Image-based atmospheric corrections - Revisited and improved, *Photogrammetric Engineering & Remote Sensing*, 62(9):1025–1036.

Chuvieco, E., 1999. Measuring changes in landscape pattern from satellite images: short-term effects of fire on spatial diversity, *International Journal of Remote Sensing*, 20:2331–2347.

Chuvieco, E. (editor), 2003. Wildland Fire Danger Estimation and Mapping: The role of remote sensing data, *Series in Remote Sensin - Volume4*. World Scientific Publishing Co. Pte. Ltd., New Jersey, 264 p.

Chuvieco, E., D. Cocero, D. Riaño, P. Martín, J. Martínez-Vega, and J. de la Riva, 2004. Combining NDVI and surface temperature for the estimation of live fuel moisture content in forest fire danger rating, *Remote Sensing of Environment*, 92:322–331.

Cohen, W.B., and T.A. Spies, 1992. Estimating structural attributes of Douglas-Fir/Western Hemlock forest stands from Landsat and SPOT imagery, *Remote Sensing of Environment*, 41:1–17

Conners, R.W., and C.A. Harlow, 1980. A theoretical comparison of texture algorithms, *IEEE Transactions on Pattern Analysis and Machine Intelligence*, Vol. PAMI-2, No. 3.

Cox, D.R., and E.J. Snell, 1989. *The Analysis of Binary Data*, Second Edition, Chapman and Hall, New York, 236 p.

Deng, Y., X., Chen, E. Chuvieco, T. Warner, and J.P. Wilson, 2007. Multi-scale linkages between topographic attributes and vegetation indices in a mountainous landscape, *Remote Sensing of Environment*, 111(1):122–134.

Earth Observation Satellite Company, 1994. *Landsat System Status Report-September 1994*, Earth Observation Satellite Company, Lanham, Maryland, 11 p.

Farina, A., 1998. *Principles and Methods in Landscape Ecology*, Chapman & Hall, London, 235 p.

Franklin, S.E., M.A. Wulder, and G.R. Gerylo, 2001. Texture analysis of IKONOS panchromatic data for Douglas-fir forest age

class separability in British Columbia, *International Journal of Remote Sensing*, 22:2627–2632.

Franklin, S.E., R.J. Hall, L. Smith, and G.R. Gerylo, 2003. Discrimination of conifer height, age and crown closure classes using Landsat-5 TM imagery in the Canadian Northwest Territories, *International Journal of Remote Sensing*, 24:1823–1834.

Haralick, R.M., K. Shanmugan, and I. Dinstein, 1973. Textural features for image classification, *IEEE Transactions on Systems, Man, and Cybernetics*, Vol. SMC-3, 6:610–621 (reprinted in *Computer Methods in Image Analysis*, IEEE Press, 1977).

Haralick, R.M., 1979. Statistical and structural approaches to texture, *Proceedings of the IEEE*, 67(5):786–804.

Helder D.L., B.L. Markham, K.J. Thome, J.A. Barsi, G. Chander, and R. Malla, 2008. Updated radiometric calibration for the Landsat-5 Thematic Mapper reflective bands, *IEEE Transactions on Geoscience and Remote Sensing*, 46:3309–3325.

Hosmer, D.W., Jr., and S. Lemeshow, 1989. *Applied Logistic Regression*, John Wiley & Sons, New York, 307 p.

Jamnick, M.S., and D.R. Beckett, 1987. A logit analysis of private woodlot owner's harvesting decisions in New Brunswick, *Canadian Journal of Forest Research*, 18:330–336.

Jia, G.J., I.C. Burke, A.F. Goetz, M.R. Kaufmann, and B.C. Kindel, 2006. Assessing spatial patterns of forest fuel using AVIRIS data, *Remote Sensing of Environment*, 102:318–327.

Kayitakire, F., C. Hamel, and P. Defourny, 2006. Retrieving forest structure variables based on image texture analysis and IKONOS-2 imagery, *Remote Sensing of Environment*, 102:390–401.

Kulakowski, D. and T.T. Veblen, 2006. *Historical Range of Variability for Forest Vegetation of the Grand Mesa National Forest, Colorado*, USDA Forest Service Final Report, Rocky Mountain Region, Colorado State University, Colorado Forest Restoration Institute, 84 p.

Li, X., and A.H. Strahler, 1985. Geometric-optical modeling of a conifer forest canopy, *IEEE Transactions on Geoscience and Remote Sensing*, 23:705–721.

Loftsgaarden, D.O., and P.L. Andrews, 1992. Constructing and testing logistic regression models for binary data: Applications to the National Fire Danger Rating System, *General Technical Report INT-286*, USDA Forest Service, Intermountain Research Station, 36 p.

Lopez, A.S., J. San-Miguel-Ayanz, and R. Burgan, 2002. Integration of satellite sensor data, fuel type maps and meteorological observations for evaluations of forest fire risk at the pan-European sale, *International Journal of Remote Sensing*, 23:713–2719.

Lozano, F.J., S. Suárez-Seoane, and E. Luis, 2007. Assessment of several spectral indices derived from multi-temporal Landsat data for fire occurrence probability modeling, *Remote Sensing of Environment*, 107(4):533–544.

Lozano, F.J., S. Suárez-Seoane, M. Nelly, and E. Luis, 2008. A multi-scale approach for modeling fire occurrence probability using satellite data and classification trees: A case study in a mountainous Mediterranean region, *Remote Sensing of Environment*, 112(3):708–719.

Lloret, F., E. Calvo, X. Pons, and R. Diaz-Delgado, 2002. Wildfires and landscape patterns in the Eastern Iberian Peninsula, *Landscape Ecology*, 17:745–759.

Maddala, G.S., 1988. *Introduction to Econometrics*, MacMillan Publishing Co., New York, 412 p.

Marceau, D.J., P.J. Howarth, J.-M.M. Dubois, and D.J. Gratton, 1990. Evaluation of the grey-level co-occurrence matrix method for land-cover classification using SPOT Imagery, *IEEE Transactions on Geoscience and Remote Sensing*, 28:513–519.

Merrill, D.F., and M.E. Alexander (editors), 1987. *Glossary of Forest Fire Management Terms*, Fourth edition, National Research Council of Canada, Canadian Committee on Forest Fire Management, Ottawa, Ontario, Canada, Publication NRCC No. 26516, 91 p.

Moreira, F., F.C. Rego, and P.G. Ferreira, 2001. Temporal (1958–1995) pattern of change in a cultural landscape of northwestern Portugal: Implications for fire occurrence, *Landscape Ecology*, 16(6):557–567.

Mutlu, M., S.C. Popescu, C. Stripling, and T. Spencer, 2007. Mapping surface fuel models using lidar and multispectral data fusion for fire behaviour, *Remote Sensing of Environment*, 112:274–285.

PCI, Inc., 1997. *Using PCI Software*, PCI Inc., Richmond Hill, Ontario, Canada.

Preisler, H.K., D.R. Brillinger, R.E. Burgan and J.W. Benoit, 2004. Probability based models for estimation of wildfire risk, *International Journal of Wildland Fire*, 13:133–142.

Price, J.C., 1987. Radiometric calibration of satellite sensors in the visible and near-infrared – History and outlook, Remote Sensing of Environment, 22:3–9.

Rao, P.V.N., M.V.R. Sesha Sai, K. Sreenivas, M.V.K. Rao, B.R.M. Rao, R.S. Dwivedi, and L. Venkataratnam, 2002. Textural analysis of IRS-1D panchromatic data for land cover classification, *International Journal of Remote Sensing*, 23:3327–3345.

Riaño, D., E. Chuvieco, F.J. Salas, A. Palacios-Orueta, and A. Bastarrika, 2002. Generation of fuel type maps from Landsat TM images and ancillary data in a Mediterranean ecosystem, *Canadian Journal of Forest Research*, 32:1301–1315.

Riaño, D., E. Chuvieco, F.J. Salas, and I. Aguado, 2003a. Assessment of different topographic corrections in Landsat-TM data for mapping vegetation types, *IEEE Transactions on Geosciences and Remote Sensing*, 41:1056–1061.

Riaño, D., E. Meier, B. Allgower, E. Chuvieco, and S.L. Ustin, 2003b. Modeling airborne laser scanning data for the spatial generation of critical forest parameters in fire behavior modeling, *Remote Sensing of Environment*, 86(2):177–186.

Romero-Calcerrada, R., and G.L.W. Perry, 2002. Landscape change pattern (1984–1999) and implications for fire incidence in the SPA Encinares del río Alberche y Cofio (Central Spain), *Forest Fire Research & Wildland Fire Safety* (D.X. Viegas, editor), Millpress, Rotterdam, 11 p.

Roselló Gimeno, R., 1994. *Catálogo Florístico y de Vegetación de la Comarca Natural del Alto Mijares (Castellón)*, Servei de Publicacions, Diputació de Castello, Castelló, 650 p.

Rothermel, R.C., 1983. How to predict the spread and intensity of forest and range fires, *General Technical Report INT-143*, USDA Forest Service, Intermountain Research Station, Ogden, Utah, 53 p.

Saatchi, S., K. Halligan, D.G. Despain, and R.L. Crabtree, 2007. Estimation of forest fuel load from radar remote sensing, *IEEE Transactions on Geoscience and Remote Sensing*, 45:1726–1740.

SAS Institute, Inc., 1999. *SAS Online Document*, Version eight, SAS Institute Inc., Cary, North Carolina.

Skowronski, N, K. Clark, R. Nelson, J. Hom, and M. Patterson, 2007. Remotely sensed measurements of forest structure and fuel loads in the Pinelands of New Jersey, *Remote Sensing of Environment*, 108:123–129.

Solberg, A.H.S., 1999. Contextual data fusion applied to forest map revision, *IEEE Transactions on Geoscience and Remote Sensing*, 37:1234–1243.

Stephens, S.L., and M.A. Finney, 2002. Prescribed fire mortality in Sierra Nevada mixed conifer tree species: Effects of crown damage and forest floor consumption, *Forest Ecology and Management*, 162:261–271.

St-Louis, V., A.M. Pidgeon, V.C. Radeloff, T.J. Hawbaker, and M.F. Clayton, 2006. High-resolution image texture as a predictor of bird species richness, *Remote Sensing of Environment*, 105:299–312.

Teillet, P.M., B. Guindon, and D.G. Goodenough, 1982. On the slope-aspect correction of multispectral scanner data, *Canadian Journal of Remote Sensing*, 8:84–106.

Tragsatec., 1996. Plan de selvicultura preventiva de incendios en los sistemas forestales de la Generalitat Valenciana, *Tragsatec*, Madrid, Inéd.

Tso, B., and P.M. Mather, 2001. *Classification Methods for Remotely Sensed Data*, Taylor and Francis, Ltd., London, 352 p.

Tuominen, S., and A. Pekkarinen, 2005. Performance of different spectral and textural aerial photograph features in multi-source forest inventory, *Remote Sensing of Environment*, 94:256–268.

Vega-García, C., P.M. Woodard, S.J. Titus, W.L. Adamowicz, and B.S. Lee, 1995. A logit model for predicting the daily occurrence of human-caused forest fires, *International Journal of Wildland Fire*, 5(2):101–111.

Vega-García, C., 2003. *Evolución del Riesgo Estructural de Incendios Forestales en la Cuenca del Río Mijares (Castellón) Mediante Indices de Ecología del Paisaje y Teledetección*, Ph.D. dissertation, University of Alcala, Alcalá, Spain, 337 p.

Vega-García, C., C. Ortiz Ruiz, R. Canet Castellà, I. Sánchez Bosch, and D. Queralt Creus, 2008. Operational application of a daily human-caused forest fire prediction model in Catalonia, *Proceedings of the Second International Symposium on Fire Economics, Planning and Policy: A Global View*, 19–22 April 2004, Córdoba, España. (USDA Forest Service, *General Technical Report PSW-GTR-208*, Pacific Southwest Research Station, Riverside, California), pp. 567–579.

Vega-García, C., and E. Chuvieco, 2006. Applying local measures of spatial heterogeneity to Landsat-TM images for predicting wildfire occurrence in Mediterranean landscapes, *Landscape Ecology*, 21:595–605.

Woodcock, C.E., and A.H. Strahler, 1987. The factor of scale in remote sensing, *Remote Sensing of Environment*, 21:311–332.

Zhai, Y.S, I.A. Munn, and D.L. Evans, 2003. Modeling forest fire probabilities in the South Central United States using FIA data, *Southern Journal of Applied Forestry*, 27:11–17.

(Received 03 February 2009; accepted 02 November 2009; final version 30 November 2009)